Faint Debris Detection by Particle based Track-before-detect Method

Masahiko Uetsuhara
The Institute of Statistical Mathematics
Norikazu Ikoma
Kyushu Institute of Technology, The Institute of Statistical Mathematics

ABSTRACT

This study aims at developing a particle method to detect faint debris, which is hardly seen in single image, from an image sequence based on a track-before-detect (TBD) method. TBD methods try to track targets without explicitly detecting the signals followed by evaluation of goodness of each track and obtaining detection results. This study proposes a particle based TBD (P-TBD) method consisting of tracking of target state and heuristic search of initial state. The target tracking is implemented by a particle filter (PF). PF is an optimal filtering technique that can estimate the target state once an initial distribution of target state is given as a prior knowledge. An evolutional algorithm (EA) is utilized to search the initial distribution. The EA iteratively evaluates goodness of initial particles for the same image sequences and resulting set of particles is used as an initial distribution of PF.

This paper designs the P-TBD method and verifies it. The P-TBD method is applied to image sequences acquired during observation campaigns dedicated to GEO breakup fragments, which would contain a sufficient number of faint debris images. The results indicate the feasibility of tracking faint debris by the proposed method.

1. INTRODUCTION

It is important for optical space surveillance system to have capabilities of tracking faint targets, i.e., dim intensity targets in an image, to monitor and characterize orbital debris population. There is a trend of realizing low cost and sustainable space surveillance system by enthusiastic supports from amateur telescopes networks [1,2]. A large part of such telescopes have relatively small apertures (0.1–1m class). For them, faint target tracking capabilities can contribute to improve coverage of orbital debris population spatially and temporally, and for large aperture telescopes the capabilities enables to characterize unseen orbital debris population. This study aims at developing a fast, scalable, and operational model to track dim intensity targets in image sequences taken by telescopes.

In the context of optical target tracking (and also Radar tracking), tracking methods can be two folds: detect-before-track (DBT) and track-before-detect (TBD). DBT methods first detect candidates of target's feature points as signals from each image and then try to associate the signals to individual tracks in an image sequence. TBD methods, on the other hand, try to track targets without explicitly detecting the shapes followed by evaluation of goodness of each track. It becomes almost impossible for DBT methods to distinguish target shapes with background as intensity of targets closes to the background level and moreover the number of signal-to-track association trials explodes in such case.

TBD methods can avoid the aforementioned problems because they do not require detection of target shapes though still require hypotheses for target tracks which usually result in increasing computational workload of testing each hypothesis. For example, the stacking method, which is a well known TBD application for debris detection purpose [3], evaluates a goodness of each hypothesis track by stacking region of interest (ROI) at each point of a testing track in each image and evaluating whether or not intensity of a target-like figure strengthens in the stacked ROI. The stacking method samples each hypothesis track uniformly from a possible region over states of track to survey all possibilities, which result in unacceptable computational workload for daily operation in actual observations at a small autonomous observatory that cannot utilize high performance computing facilities. To make it operational, the stacking method algorithm has been implemented onto the field programmable gate array (FPGA) board [4]. Considering upcoming trend of applying complementary metal-oxide-semiconductor (CMOS) image sensor to the debris observation [5], it will be necessary to develop a new algorithm that can process one hundreds times images over those taken by conventional charge-coupled device (CCD) image sensor.

This paper proposes a particle based TBD (P-TBD) method that can improve the stacking method algorithm and bring scalability to it. The basic idea of the P-TBD method is to evaluate goodness of tracks by using conditional probability distribution $p(\bullet|\bullet)$ approximated by particles, i.e., samples. The P-TBD method describes target's state as a conditional probability distribution form so that we can make use of Bayesian techniques such as optimal filtering and evolutional algorithms to characterize and track target state.

2. TRACK-BEFORE-DETECT MODELING

This section describes how to design the P-TBD method. First of all, state vector $\mathbf{x}_k$ is introduced to represent a state of a target at time t_k when kth image is acquired. The state vector $\mathbf{x}_k$ consists of target's position (x_k, y_k), magnitude of velocity s_k, and angle of velocity θ_k of the kth image as shown in Eq. 1 and Fig. 1.

$$\mathbf{x}_k = \begin{bmatrix} x_k & y_k & s_k & \theta_k \end{bmatrix}' \tag{1}$$

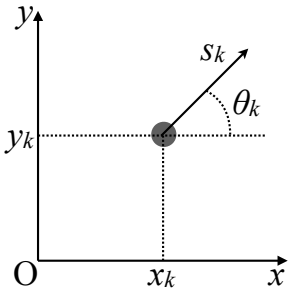

Fig. 1. State vector definition

The state vector follows a state space model that consists of the system model $\mathbf{f}(\bullet)$, the observation model $h(\bullet)$. The system model $\mathbf{f}(\bullet)$ describes time evolution of the state vector $\mathbf{x}_k$ assuming motion of target is linear during the time step $\Delta t_k = t_k - t_{k-1}$ as follows.

$$\mathbf{x}_k = \mathbf{f}(\mathbf{x}_{k-1}, \mathbf{v}_k) \tag{2}$$

The system model $\mathbf{f}(\bullet)$ consists of the following equations.

$$\begin{aligned} x_k &= x_{k-1} + \Delta t_k s_{k-1} \cos\theta_{k-1} + v_{x,k} \\ y_k &= y_{k-1} + \Delta t_k s_{k-1} \sin\theta_{k-1} + v_{y,k} \\ s_k &= s_{k-1} + v_{s,k} \\ \theta_k &= \theta_{k-1} + v_{\theta,k} \end{aligned} \tag{3}$$

where $\mathbf{v}_k = [v_{x,k}\ v_{y,k}\ v_{s,k}\ v_{\theta,k}]'$ denotes the system noise vector that follows a Gaussian distribution $N(\bullet,\bullet)$ of zero mean vector $\mathbf{0}$ and diagonal covariance matrix $\mathbf{Q} = \mathrm{diag}[\tau_x^2\ \tau_y^2\ \tau_s^2\ \tau_\theta^2]$, $N(\mathbf{0},\mathbf{Q})$. The position noises $v_{x,k}\ v_{y,k}$ deal with unsteadiness of target's image position due to environmental disturbances, whereas the velocity noises $v_{s,k}\ v_{\theta,k}$ deal with the uncertainty of linear motion assumption. To start propagation of the state vector using the system model, an initial state $\mathbf{x}_0$ be generated by a initial distribution $p(\mathbf{x}_0)$. The P-TBD method tries to discover a proper initial distribution $p(\mathbf{x}_0)$ by using an evolutional algorithm as will be described later.

The observation model, $h(\mathbf{y}_k|\mathbf{x}_k)$, evaluates a likelihood of the state vector $\mathbf{x}_k$ for the kth image $\mathbf{y}_k$. It consists of a product of three likelihood functions $h_{\bullet}(\bullet)$.

$$h(\mathbf{y}_k|\mathbf{x}_k) = h_{int}(\mathbf{y}_k|\mathbf{x}_k) \times h_{grd}(\mathbf{y}_k|\mathbf{x}_k) \times h_{spd}(\mathbf{x}_k) \tag{4}$$

First two functions evaluate intensity values of a target ROI at kth image by applying the likelihood functions for dim intensity targets introduced in [6]. Profile of the target ROI is specified in Fig. 2. $ROI_{in,k}(x_k,y_k,w)$ is a square of width w at a position (x_k,y_k). $ROI_{ou,k}(x_k,y_k,w,w_o)$ is a squared frame of thickness w_o surrounding $ROI_{in,k}$.

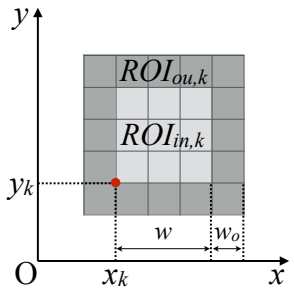

Fig. 2. Profile of target ROI on the *k*th image

The first function, $h_{int}(\mathbf{y}_k|\mathbf{x}_k)$, evaluates the mean intensity of $ROI_{in,k}$, denoted by $d_{in,k}$. The second function, $h_{grd}(\mathbf{y}_k|\mathbf{x}_k)$, evaluates the gradient of the mean intensities of $ROI_{in,k}$ and $ROI_{ou,k}$, denoted by Δd_k. The third function, $h_{spd}(\mathbf{x}_k)$, evaluates the speed of the target. The content of each likelihood function is a linear function $q_{\bullet}(\bullet)$ that maps a given value to the range from 0 to 1 with thresholds as specified in Eq. 5 and Fig. 3.

$$h_{int}(\mathbf{y}_k|\mathbf{x}_k) = q_{int}(d_{in,k}) \tag{5.1}$$

$$h_{grd}(\mathbf{y}_k|\mathbf{x}_k) = q_{grd}(\Delta d_k) \tag{5.2}$$

$$h_{spd}(\mathbf{x}_k) = q_{spd}(s_k) \tag{5.3}$$

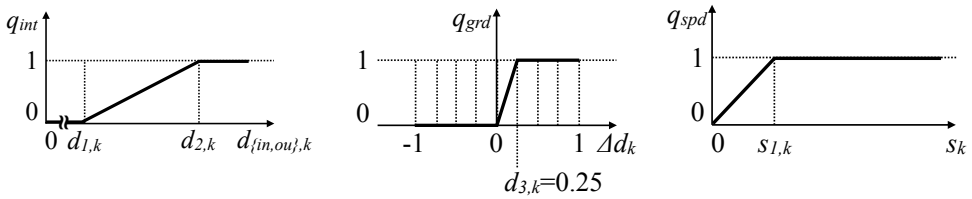

Fig. 3. Mapping functions

The mean intensity $d_{in,k}$ appeared in Eq. 5.1 is calculated by

$$d_{in,k} = avg\left[ROI_{in,k}(x_k, y_k, w)\right] \tag{6}$$

where the function $avg[\bullet]$ calculates the mean of pixel intensity values of given ROI. Again, the mean intensity gradient Δd_k appeared in Eq. 5.2 is calculated by

$$\Delta d_k = q_{int}(d_{in,k}) - q_{int}(d_{ou,k}), \quad d_{ou,k} = avg\left[ROI_{ou,k}(x_k, y_k, w, w_o)\right] \tag{7}$$

The intensity thresholds for q_{int} and q_{grd} of *k*th image, denoted by $d_{1,k}$, $d_{2,k}$, and $d_{3,k}$, are determined by using the inverse cumulative distribution function of pixel intensities over *k*th image, denoted by $\text{CDF}^{-1}\mathbf{y}_k(\bullet)$. A Gaussian distribution is generally a good approximation of the pixel intensity distribution over the image that is preprocessed by the basic image reductions such as bias correction and limb darkening correction. In this paper, $d_{1,k}$ is determined around the cumulative probability at $\mu+\sigma$, i.e., $d_{1,k} \approx \text{CDF}^{-1}\mathbf{y}_k(84.13\%)$, and $d_{2,k}$ is determined around the cumulative probability at $\mu+2\sigma$, i.e., $d_{2,k} \approx \text{CDF}^{-1}\mathbf{y}_k(97.73\%)$, whereas $d_{3,k}$ is set at a quartile point of $q_{int}(\bullet)$, thus $d_{3,k}=0.25$. The speed thresholds of q_{spd} are designed by assuming that very slow targets will not likely to have high intensity values such that h_{spd} acts like a weak constraint over h_{int} and h_{grd}. The thresholds of q_{int}, q_{grd}, and q_{spd} should be slightly tuned with optical sensor characteristics and weather conditions during observations. Actual threshold values in this study are given in the section 3.

In the P-TBD method, a target-tracking algorithm and an initial state search algorithm are introduced to solve the state space model. The target-tracking algorithm is implemented by a particle filter (PF) [7]. The PF is an optimal filtering technique that can estimate state vector at a time t_k once an initial state $\mathbf{x}_0$ is obtained from an initial distribution $p(\mathbf{x}_0)$. An evolutional algorithm (EA) is applied to search the initial distribution $p(\mathbf{x}_0)$. The EA iteratively applies propagation and likelihood evaluation of particles for the same image sequences and resulting set of particles is used as an initial distribution of the PF. The PF and the EA can evaluate nonlinear probability distribution directly so that we can track dim intensity targets without specifying target's feature points beforehand. Each of target tracking and initial state search algorithms is detailed in the following subsections.

2.1 Target-Tracking Algorithm

The PF sequentially evaluates predictive distribution and filter distribution of target state vector $\mathbf{x}$ at each time, i.e., at each image. The predictive distribution, denoted by $p(\mathbf{x}_k|\mathbf{y}_{1:k-1})$, is a conditional probability distribution of state vector $\mathbf{x}_k$ given a set of sequential images $\mathbf{y}_{1:k-1}\equiv\{\mathbf{y}_1, \mathbf{y}_2, \ldots, \mathbf{y}_{k-1}\}$ at time t_k. The predictive distribution $p(\mathbf{x}_k|\mathbf{y}_{1:k-1})$ is now represented by an ensemble of N predictive particles sampled from $p(\mathbf{x}_k|\mathbf{y}_{1:k-1})$.

$$\left\{\mathbf{x}_{k|k-1}^{(i)}\right\}_{i=1}^{N} = \left\{\mathbf{x}_{k|k-1}^{(1)}, \mathbf{x}_{k|k-1}^{(2)}, ..., \mathbf{x}_{k|k-1}^{(N-1)}, \mathbf{x}_{k|k-1}^{(N)}\right\}, \quad \mathbf{x}_{k|k-1}^{(i)} \sim p(\mathbf{x}_k|\mathbf{y}_{1:k-1}) \tag{8}$$

When we acquire a new image $\mathbf{y}_k$ in addition to $\mathbf{y}_{1:k-1}$, we can evaluate the filter distribution, denoted by $\mathbf{x}_{k|k}\equiv p(\mathbf{x}_k|\mathbf{y}_{1:k})$. Likewise the filter distribution $p(\mathbf{x}_k|\mathbf{y}_{1:k})$ is now represented by an ensemble of N filter particles sampled from $p(\mathbf{x}_k|\mathbf{y}_{1:k})$

$$\left\{\mathbf{x}_{k|k}^{(i)}\right\}_{i=1}^{N} = \left\{\mathbf{x}_{k|k}^{(1)}, \mathbf{x}_{k|k}^{(2)}, ..., \mathbf{x}_{k|k}^{(N-1)}, \mathbf{x}_{k|k}^{(N)}\right\}, \quad \mathbf{x}_{k|k}^{(i)} \sim p(\mathbf{x}_k|\mathbf{y}_{1:k}) \tag{9}$$

The following paragraphs explain how to evaluate each of the predictive particles and the filter particles.

Predictive particles are described by the system model $\mathbf{f}(\bullet)$. The system model propagates the filtered particles evaluated at previous time t_{k-1}, $\mathbf{x}_{k-1|k-1}^{(i)}$, to the current time t_k to make predictive particles $\mathbf{x}_{k|k-1}^{(i)}$. That is

$$\mathbf{x}_{k|k-1}^{(i)} = \mathbf{f}(\mathbf{x}_{k-1|k-1}^{(i)}, \mathbf{v}_k^{(i)}) \tag{10}$$

where $\mathbf{v}_k^{(i)}$ is the ith particle's system noise at time t_k.

Filter particles are computed by the observation model $h(\bullet)$. The observation model evaluates likelihood value, β, of each predictive particle at time t_k with respect to observation at the same time, thus denoted by a conditional probability distribution of $\mathbf{y}_k$ given $\mathbf{x}_{k|k-1}$.

$$\beta_k^{(i)} = h(\mathbf{y}_k|\mathbf{x}_{k|k-1}^{(i)}) \tag{11}$$

Once the likelihood value for each particle, $\beta_k^{(i)}$, is calculated, it is normalized with respect to the sum of likelihood values of all particles to get a weight of each particle, denoted by $\gamma_k^{(i)}$.

$$\gamma_k^{(i)} = \frac{\beta_k^{(i)}}{\sum_{i=1}^{N}\beta_k^{(i)}} \tag{12}$$

Filter distribution is now approximated by weighed predictive particles such that

$$p(\mathbf{x}_k|\mathbf{y}_{1:k}) \approx \sum_{i=1}^{N}\gamma_k^{(i)}\delta(\mathbf{x}_{k|k-1} - \mathbf{x}_{k|k-1}^{(i)}) \tag{13}$$

where $\delta(\bullet)$ is the Dirac delta function that returns 1 when $\delta(\mathbf{0})$ otherwise 0. We get N filter particles by resampling predictive particles for N times according to the filter distribution expressed in the right side of Eq. 13. When implementing resampling code, one should calculate the inverse cumulative distribution function of the approximated filter distribution ($\text{CDF}^{-1}\mathbf{x}_{k|k}$) and conduct stratified sampling to draw N particles from $\text{CDF}^{-1}\mathbf{x}_{k|k}$.

2.2 Initial State Search Algorithm

It is necessary to prepare the initial particles $\mathbf{x}_{0|0}^{(\bullet)}$, which represent the initial distribution, in some way to start the target tracking. The predictive/filter particles may not track a target in the target tracking process if the initial particles are sparsely sampled from the initial distribution around the target due to lack of prior information about the target. This paper applies an EA to conduct a heuristic search of a reasonable initial distribution.

The EA repeats search of a conditional probability distribution of $\mathbf{x}_{0|0}$ given T sequential images $\mathbf{y}_{1:T}$. In the EA, the initial particles at lth search $\mathbf{x}_{E,l}^{(i)}$ consist of N_N new particles $\mathbf{x}_{N,l}^{(n)}$ and N_S surviving particles $\mathbf{x}_{S,l}^{(m)}$ as follows.

$$\left\{\mathbf{x}_{E,l}^{(i)}\right\}_{i=1}^{N_E} = \left\{\left\{\mathbf{x}_{N,l}^{(n)}\right\}_{n=1}^{N_N}, \left\{\mathbf{x}_{S,l}^{(m)}\right\}_{m=1}^{N_S}\right\} \tag{14}$$

At the beginning of the first search l=0 the initial particles only consists of the new particles, that is

$$\left\{\mathbf{x}_{E,0}^{(i)}\right\}_{i=1}^{N_E} = \left\{\mathbf{x}_{N,0}^{(n)}\right\}_{n=1}^{N_E} \tag{15}$$

When one terminates the initial state search after L searches to start the target tracking, an ensemble of N_S surviving particles are applied to denote the initial particles of the target-tracking algorithm, thus N=N_S.

$$\left\{\mathbf{x}_{0|0}^{(i)}\right\}_{i=1}^{N} = \left\{\mathbf{x}_{S,L}^{(i)}\right\}_{i=1}^{N_S} \tag{16}$$

The following sections explain how to evaluate the new particles and the surviving particles in a search.

The new particles are sampled from a probability distribution with wide hypothesis range, whereas the surviving particles are sampled from a conditional probability distribution of $\mathbf{x}_{E,l\text{-}1}$ given $\mathbf{y}_{1:T}$, $p(\mathbf{x}_{E,l\text{-}1}|\mathbf{y}_{1:T})$, by roughly evaluating a goodness of each initial particle's track at l-1th search. It may be noted that random sampling is better than stratified sampling for the EA's sampling process to preserve a diversity of initial particles.

Each element of nth new particle $\mathbf{x}_{N,l}^{(n)}=[x_{N,l}^{(n)}\ y_{N,l}^{(n)}\ s_{N,l}^{(n)}\ \theta_{N,l}^{(n)}]'$ is sampled from an uniform probability distribution of a given range U(•,•) as follows.

$$\begin{aligned} x_{N,l}^{(n)} &\sim U(\epsilon_{x1}, \epsilon_{x2}) \\ y_{N,l}^{(n)} &\sim U(\epsilon_{y1}, \epsilon_{y2}) \\ s_{N,l}^{(n)} &= \epsilon_s\sqrt{u}, \quad u \sim U(0,1) \\ \theta_{N,l}^{(n)} &\sim U(\epsilon_{\theta 1}, \epsilon_{\theta 2}) \end{aligned} \tag{17}$$

Each element of mth surviving particle $\mathbf{x}_{S,l}^{(m)}=[x_{S,l}^{(m)}\ y_{S,l}^{(m)}\ s_{S,l}^{(m)}\ \theta_{S,l}^{(m)}]'$ is generated by a combination of a raw surviving particle $\mathbf{x}_{S^*,l}^{(m)}=[x_{S^*,l}^{(m)}\ y_{S^*,l}^{(m)}\ s_{S^*,l}^{(m)}\ \theta_{S^*,l}^{(m)}]'$ sampled from the conditional probability distribution of the initial distribution at the previous search $p(\mathbf{x}_{E,l\text{-}1}|\boldsymbol{y}_{1:T})$ and a perturbation particle $\boldsymbol{v}_l^{(m)}=[v_{x,l}^{(m)}\ v_{y,l}^{(m)}\ v_{s,l}^{(m)}\ v_{\theta,l}^{(m)}]'$ following a Gaussian distribution N($\mathbf{0}$, $\mathbf{Q}_0$) where $\mathbf{Q}_0$=diag[$\tau_{x0}^2\ \tau_{y0}^2\ \tau_{s0}^2\ \tau_{\theta 0}^2$].

$$\mathbf{x}_{S*,l}^{(m)} \sim p(\mathbf{x}_{E,l-1}|\mathbf{y}_{1:T}) \tag{18.1}$$

$$\begin{aligned} x_{S,l}^{(m)} &= x_{S*,l}^{(m)} + v_{x,l}^{(m)} \\ y_{S,l}^{(m)} &= y_{S*,l}^{(m)} + v_{y,l}^{(m)} \\ s_{S,l}^{(m)} &= s_{S*,l}^{(m)} + v_{s,l}^{(m)} \\ \theta_{S,l}^{(m)} &= \theta_{S*,l}^{(m)} + v_{\theta,l}^{(m)} \end{aligned} \tag{18.2}$$

It is necessary to evaluate the conditional probability distribution $p(\mathbf{x}_{E,l\text{-}1}|\mathbf{y}_{1:T})$ in Eq. 18.1 to conduct sampling of $\mathbf{x}_{S^*,l}^{(\bullet)}$. The EA computes $p(\mathbf{x}_{E,l\text{-}1}|\mathbf{y}_{1:T})$ by using an analogy from the PF's likelihood evaluation such that

$$p(\mathbf{x}_{E,l-1}|\mathbf{y}_{1:T}) \approx \sum_{i=1}^{N_E} \gamma_{1:T,l-1}^{(i)} \delta(\mathbf{x}_{E,l-1} - \mathbf{x}_{E,l-1}^{(i)}) \tag{19}$$

where the weight of ith initial particle at l-1th search is denoted by $\gamma_{1:T,l\text{-}1}^{(i)}$. Each weight is gained by normalizing the likelihood value $\beta_{1:T,l\text{-}1}^{(\bullet)}$ by the same evaluation process as in Eq. 12. The likelihood value of ith initial particle $\beta_{1:T,l\text{-}1}^{(i)}$ is evaluated by using an analogy from Eq. 11 such that

$$\beta_{1:T,l-1}^{(i)} = \sum_{k=1}^{T} h(\mathbf{y}_k|\mathbf{x}_{E,l-1,k}^{(i)}) \tag{20}$$

The position of ith initial particle at kth image, $(x_{E,l\text{-}1,k}^{(i)}, y_{E,l\text{-}1,k}^{(i)})$, is evaluated by assuming that target's motion is linear during the entire image sequence $\mathbf{y}_{1:T}$.

$$\begin{aligned} x_{E,l-1,k}^{(i)} &= x_{E,l-1,1}^{(i)} + (t_k - t_1) s_{E,l-1}^{(i)} \cos\theta_{E,l-1}^{(i)} \\ y_{E,l-1,k}^{(i)} &= y_{E,l-1,1}^{(i)} + (t_k - t_1) s_{E,l-1}^{(i)} \sin\theta_{E,l-1}^{(i)} \end{aligned} \tag{21}$$

3. EXPERIMENTAL SETUP

This section arranges an experiment to verify P-TBD's basic feasibility to track a dim intensity target. In this experiment, P-TBD is applied to several image sequences in which presence of dim targets has been confirmed by using the FPGA-based stacking method [4]. The experiment consists of two parts. The first experiment is verification of the target-tracking algorithm. The second experiment is verification of the initial state search algorithm.

3.1 Test Image Sequences

Three image sequences are applied to the experiments. The image sequences are taken on 21 October 2011 in the observation campaign to survey breakup fragments in the geostationary region. The sensor used to acquire the image sequences is operated by the TAOS project. The sensor is located at the National Central University Lulin

Observatory in Taiwan. The sensor consists of 50-cm aperture telescope and 2 k by 2 k cooled CCD, with a field-of-view of 1.74° by 1.78° which approximately equals to 3 arcsec/px (pixel) resolution. Each image sequence consists of 29 images. Each image is taken with 5.90 sec exposure time and 2.66 sec readout time. Basic image reduction including limb-darkening correction, bias correction, and bright stars masking are applied to each image sequence prior to the experiments.

3.2 Experimental Condition

This subsection describes main conditions of the two experiments: 1) the target tracking verification and 2) the initial state search verification. Each experiment applies same values for threshold parameters of the likelihood functions, and ROI of each particle. The likelihood function parameters are $[d_{1,k}\ d_{2,k}\ d_{3,k}\ s_{1,k}]'=[\mathrm{CDF}^{-1}\mathbf{y}_k(97.5\%)\ \mathrm{CDF}^{-1}\mathbf{y}_k(99.2\%)\ 0.25\ 3.0\text{px/frame}]'$ and the ROI parameters are $[w\ w_0]'=[3\text{px}\ 1\text{px}]'$. Also, each experiment is conducted over a local image (LI) sequence. The LI is a part of an image and its region is same for every image of the image sequence. The purpose of considering LI over each image sequence is to confirm P-TBD's capability of single target tracking. A region of LI of each image sequence is manually determined to hold a target within the LI. The specifications of each target and its LI in image sequence are summarized in Table 1.

Table 1. Specifications of the targets

Name	Visual Magnitude	Position at first image $x_{0,true}$; $y_{0,true}$ [px]	Velocity of target s_{true} [px/frame]; θ_{true} [deg]	Region of LI in each image x; y; width; height [px]
Target 1	16.70	1875; 837	1.96; 284.8	1700; 700; 300; 300
Target 2	17.68	629; 709	3.86; 287.8	500; 500; 300; 300
Target 3	18.22	1077; 1901	3.19; 337.3	1000; 1700; 300; 300

Each experiment is mainly differentiated by the initial distribution definition. The objective of the experiment 1 is to confirm that the target-tracking algorithm is capable of track a target by using a proper initial distribution that contains target's information. In the initial distribution of the experiment 1, uncertainty of the initial position (x_0 and y_0) is limited to target proximity; x_0 and y_0 are sampled from the uniform distribution with ±10 px range around a target's true position on the first image ($x_{0,true}$ and $y_{0,true}$ as specified in Table 1). That is $x_0 \sim \mathrm{U}(x_{0,true}\text{-}10\text{px}, x_{0,true}\text{+}10\text{px})$ and $y_0 \sim \mathrm{U}(y_{0,true}\text{-}10\text{px}, y_{0,true}\text{+}10\text{px})$. Whereas the initial velocity components (s_0 and θ_0) do not intensively apply target information; s_0 is sampled using Eq. 18 with ε_s=15 px/frame and θ_0 is sampled as $\theta_0 \sim \mathrm{U}(0\text{deg}, 360\text{deg})$. The objective of the experiment 2, on the other hand, is to confirm that initial state search algorithm is capable of finding a proper initial distribution to track a target by the target-tracking algorithm. To do this, the initial distribution of new particles of the initial state search algorithm applies a wide uncertainty to the initial position range (ε_{x1}, ε_{x2}, ε_{y1}, ε_{y2}) to cover the entire region of LI in addition to applying wide uncertainties to s_0 and θ_0 with same values as the experiment 1. The magnitude of initial state's uncertainty is different between the experiments so that the experiment 1 uses 10,000 particles in the target-tracking, while the experiment 2 uses 20,000 new particles and 80,000 surviving particles in the initial state estimation with a maximum of 20 searches (i.e., l = 1, 2, … 19, 20) and the whole surviving particles are inherited to the target-tracking. It is noted that the PF's system noise parameters for the experiment 1 and 2 are $[\tau_x\ \tau_y\ \tau_s\ \tau_\theta]'=[1.0\text{px}\ 1.0\text{px}\ 0.5\text{px/frame}\ 0.5\text{deg}]'$ and the EA's surviving particles parameters for the experiment 2 are $[\tau_x\ \tau_y\ \tau_s\ \tau_\theta]'=[1.0\text{px}\ 1.0\text{px}\ 1.0\text{px/frame}\ 1.0\text{deg}]'$.

As the final part of the experimental setup, the image sequences after the image reduction are shown in Fig. 4 and Fig. 5. Fig. 4 depicts the time series of target proximity images cut from LI sequences whereas Fig. 5 shows the whole LI at the first frame of each image sequence for example. The brightness range of the example images is equivalent to the brightness thresholds at each frame ($d_{1,k}$ and $d_{2,k}$), thus completely black pixel represents the brightness of $d_{1,k}$ or darker and completely white pixel represents the brightness of $d_{2,k}$ or brighter.

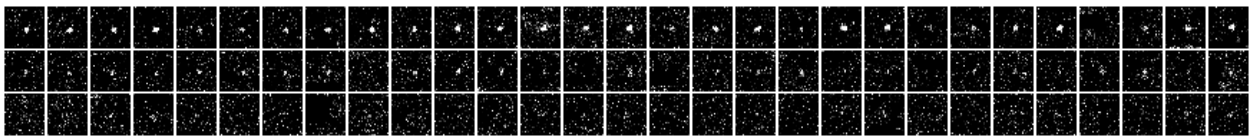

Fig. 4. Time series of target proximity images (1st row: Target 1, 2nd row: Target 2, 3rd row: Target 3)

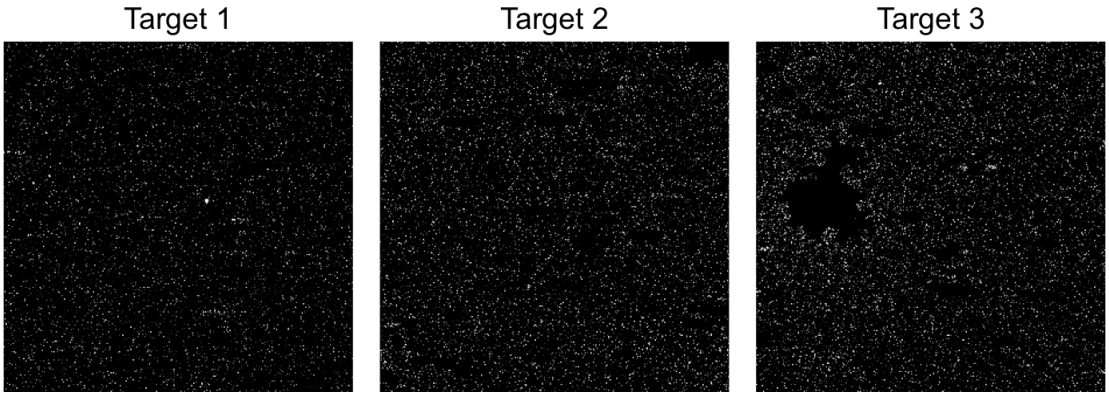

Fig. 5. The first LI of each image sequence

4. RESULT AND DISCUSSION

This section shows results of each experiment and discusses the feasibilities of a single target tracking and the target's initial state search by using the P-TBD. The results and the discussions focus on the estimation performance of target's position in each image.

4.1 Experiment 1: Target Tracking Verification

The evolutions of filter distributions of target's positions during image sequences are shown in Fig. 6. Size of each frame corresponds to the region of LI of each image sequence. At each frame, the filter distribution is plotted as a histogram of positions of whole filter particles (i.e., 10000 particles) on the image plane. Each filter particle adds a scalar value 1.0 onto each of the pixels within the particle's ROI (i.e., the 3px by 3px around the particle's position) of the histogram to represent the filter particle's position. In each histogram, a color map is applied to the value of each histogram bin so that black is applied to the minimum value and the color shifts from violet to red to orange and yellow is applied to the maximum value.

At the first frame of each image sequence, the filter distribution appears around the target proximity because of the initial distribution of position components described in the previous section. At the beginning phase of the target tracking, the filter distribution spread around the target in each image sequences due to the uncertainties of velocity components. As the frame proceeds, the filter distribution converges around the target by the particles' transition that the spread particles gradually disappear and particles increase around the target's position. The timing of the convergence of the filter distribution of the target 1 is the earliest, and that of the target 3 is the latest. It can be supposed that dimmer target requires longer image sequence to get a consistent result. The evolution of the filter distributions of the target 2 shows an interesting phenomenon during the middle period of the image sequence (k = 15,…,20). During this period, convergence of filter distribution gets worse. After this period, the filter distribution converges again. This phenomenon can be also confirmed for the last several frames of the target 1. It supposed to be related with the temporal variation of the target's brightness that can be confirmed in Fig. 4.

Fig. 7 plots the estimation error of the target's position as the difference between estimated position (x_{est}, y_{est}) and the target's true position (x_{true}, y_{true}) at each frame. The estimated positions are evaluated by two forms; the one is the average of whole particles positions, i.e., (x_{est}, y_{est})=(x_{avg}, y_{avg}), and the other is the position of the maximum value bin at the filter particles histogram, i.e., (x_{est}, y_{est})=(x_{max}, y_{max}). The estimation error of both of (x_{avg}, y_{avg}) and (x_{max}, y_{max}) shows good precision when the filter distribution is converged. Difference of them can be seen at the transition phases of the filter distribution. At the transition phases, the position of the maximum value bin (x_{max}, y_{max}) tends to be sensitive to the true target position.

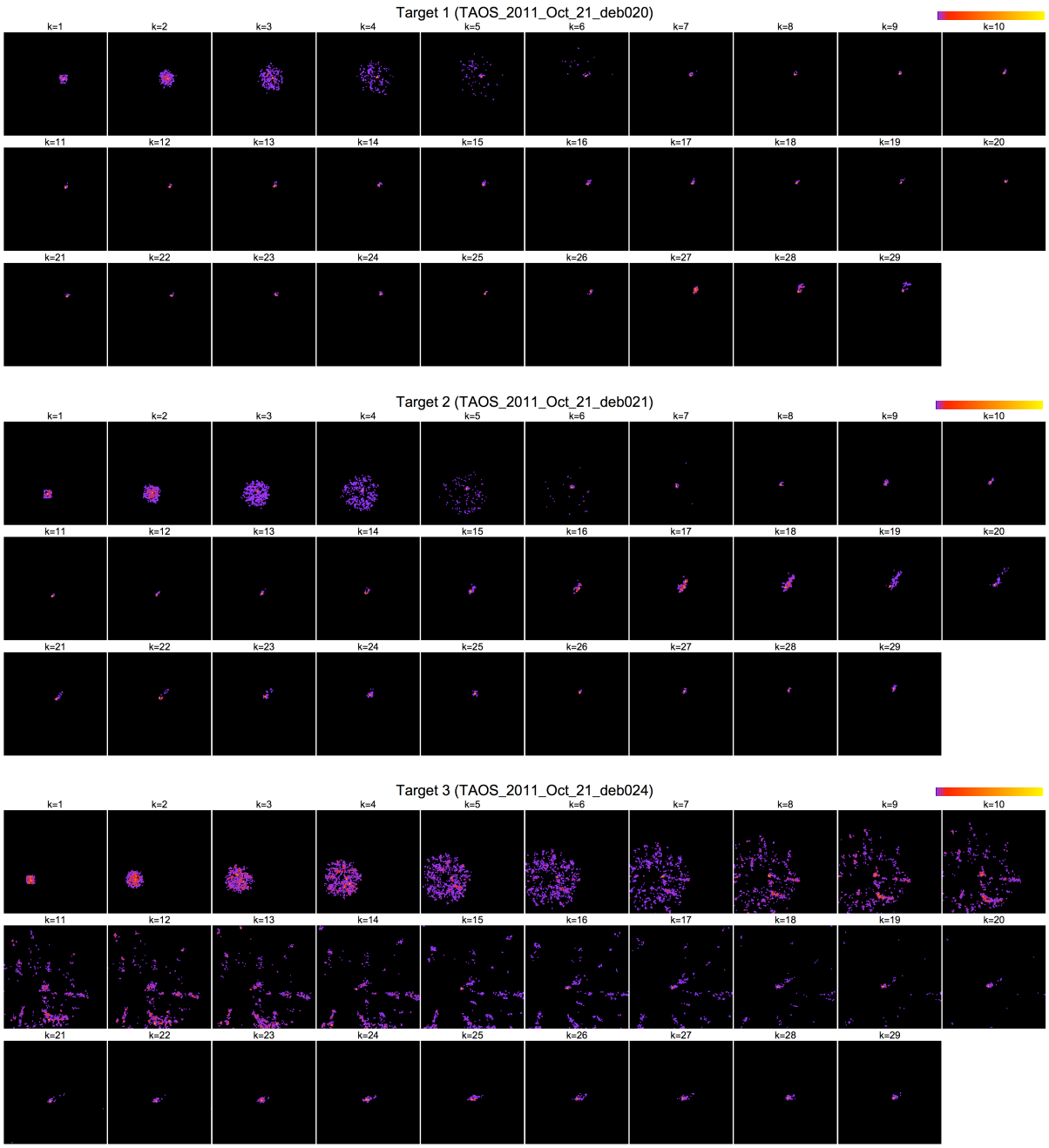

Fig. 6. Transition of filter distributions of target positions

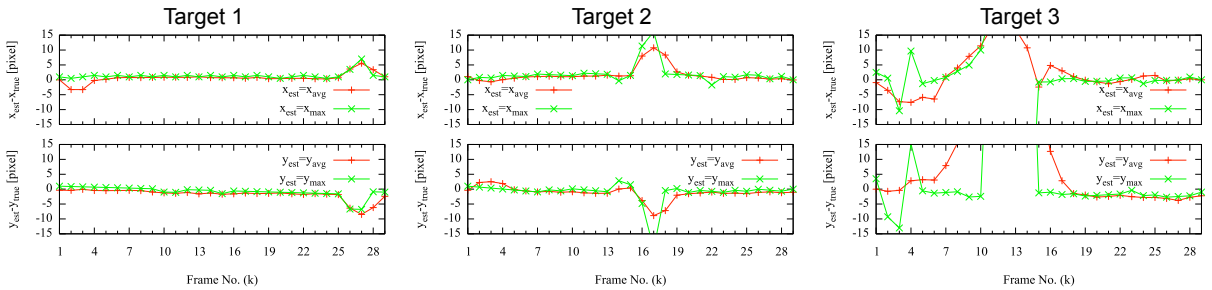

Fig. 7. Estimation error of target positions

4.2 Experiment 2: Initial State Search Verification

The initial distribution of each target's position after l searches (l=1,5,10,15,20) is shown in Fig. 8 to represent the evolution of the initial distribution. Each initial distribution is visualized by the same manner as the filter distribution's visualization in the experiment 1. In this experiment, the peak regions colored in orange-yellow gradation represents the possible initial positions of a target.

At the first search, the initial state search algorithm does not capture the target's initial position. As the algorithm repeats the search, it discovers many peak regions that may be correlated with the target's initial position. The number of peak regions decreases as the search proceeds. The transition of such peak regions is the earliest in the case of the target 1 and the latest in the case of the target 3. The initial distribution of each target after 20 searches captures a true target's region though several false regions remains in the case of the target 2 and the target 3.

Initial distributions after 10 searches and 20 searches are applied to the target-tracking algorithm to confirm whether or not the target is tracked by using the initial distributions. Fig. 9 plots the estimation error of the target's position by the same manner in the experiment 1. With the initial distribution after 10 searches, the target 1 is well tracked from beginning to end and the target 3 is also tracked in the latter half period however the target 2 is lost in the latter half period. In the case of target 2, several false peak regions are located around the true region so that the false regions may affect the target tracking. With the initial distribution after 20 searches, every target is well tracked with the same tendency as the experiment 1 because true target's position is specified in the initial distribution.

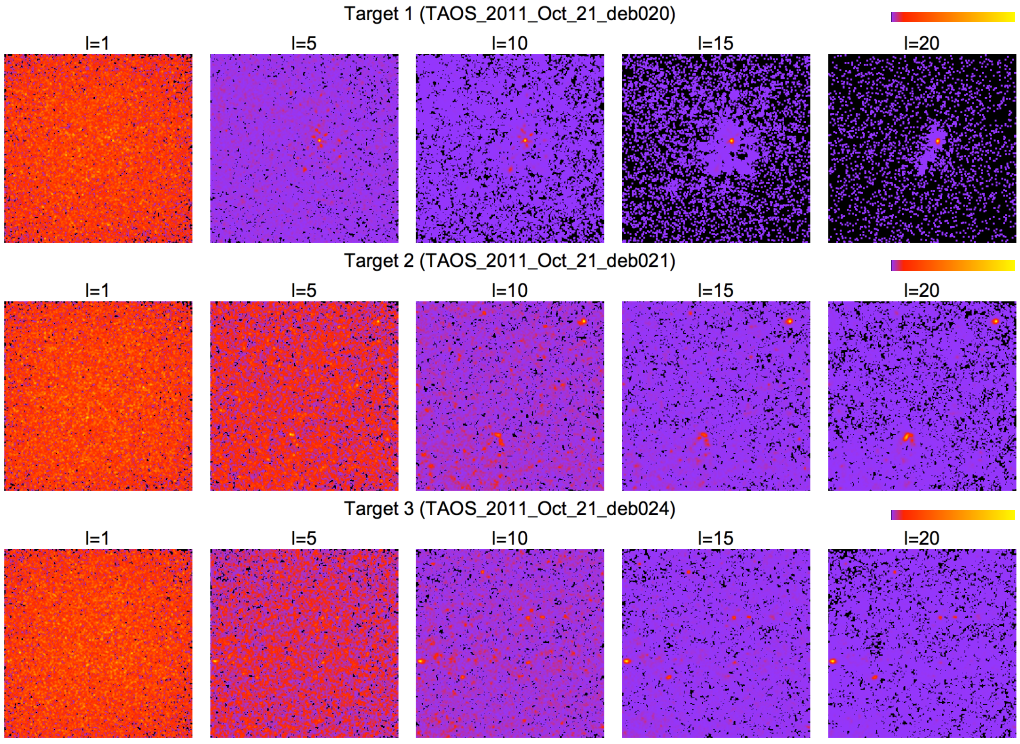

Fig. 8. Transition of initial state distributions of target positions

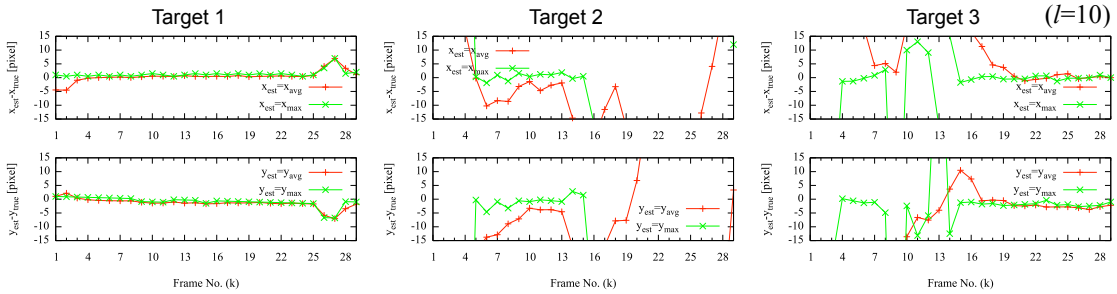

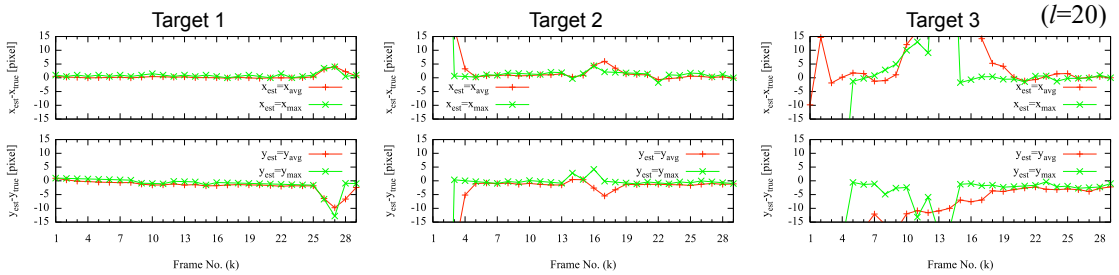

Fig. 9. Estimation error of target positions in the target tracking using the initial distributions after *l* searches

5. CONCLUSION

This paper proposed a TBD method to track dim intensity space objects in image sequences. The TBD method named P-TBD was designed based on the state space model, which was solved by the target-tracking algorithm and the initial state search algorithm. In the target-tracking algorithm a particle filter was applied to solve the state space model to track targets sequentially. In the initial state search algorithm an evolutional algorithm was applied to based on the modified state space model to heuristically discover a proper initial distribution of targets.

Feasibility of tracking dim targets by using P-TBD is confirmed by two experiments. In the first experiment, it is confirmed that P-TBD is capable of tracking a single target if a target's prior information about the initial position on the image sequence is considered before starting the target tracking. In the second experiment, it is confirmed that P-TBD can acquire the target's prior information for oneself in offline and the acquired initial distribution is valid to conduct the target tracking. For advancing the P-TBD to the real operational level, intensive studies will go on to expand the capability of P-TBD in more complicated situations.

ACKNOWLEDGEMENT

The authors wish to acknowledge Dr. Toshifumi Yanagisawa for providing the image sequences for this study. Grateful acknowledgement is given to Dr. Andrew Wang for coordinating the TAOS telescope's operation in the observation campaign. This study is supported by JSPS KAKENHI Grant Number 26820374.

REFERENCES

1. Molotov, I. et al, International Scientific Optical Network for Space Debris Research, Advances in Space Research, Vol. 41, No. 7, 1022-1028, 2008.
2. http://www.spaceviewnetwork.com; accessed on 7 Sep. 2014.
3. Yanagisawa, T. et al, "The Stacking Method": the Technique to Detect Small Size of GEO Debris and Asteroids, Japan Aerospace Exploration Agency, JAXA-RR-07-032E, 2008.
4. Yanagisawa, T., and Kurosaki, H., Detection of Faint GEO Objects using JAXA's Fast Analysis Methods, Transactions of the Japan Society for Aeronautical and Space Sciences, Aerospace Technology Japan, Vol. 10, 29-35, 2012.
5. Schildknecht, T. et al, Improved Space Object Observation Techniques using CMOS Detectors, Proceedings of the 6th European Conference on Space Debris, 22-27, Darmstadt, Germany, 2013.
6. Ikoma, N., On a Particle Filter based Visual Tracking over Dim Intensity Image having out of Field-Of-View, The International Workshop on Advanced Computational Intelligence and Intelligent Informatics, #07, Fukui, Japan, 2014.
7. Kitagawa, G., Monte Carlo Filter and Smoother for Non-Gaussian Nonlinear State Space Models, Journal of computational and graphical statistics, Vol. 5, No. 1., 1-25, 1996.